CAFE60v1: The CSIRO Climate re-Analysis Forecast Ensemble system

T. J. O'Kane, P. A. Sandery, V. Kitsios, P. Sakov, M.A. Chamberlain, M.A. Collier, D.T. Squire, C. R.J. Matear, Chapman S. Schroeter, I. Watterson, D. Harries, B. Sloyan, T. Moore + DCFP

"Multi-annual to Decadal Climate Predictability in the North Atlantic-Arctic Sector" Sept 20-22
www.csiro.au

CSIRO

Motivation:

CAFE60 was developed to

- provide the first ensemble reanalysis of the climate over the past 60 years of sufficient size and temporal resolution that the evolving climate pdf might be accurately estimated
- generate self consistent and balanced initial conditions for O(100) forecasts each month from 1960 to present
- as part of the WMO Grand Challenge in Near Term Climate Prediction to develop an operational system capable of generating outputs sufficient to meet the conditions to become a WMO santioned global data producing centre (GDPC)
- push the boundaries of data assimilation - i.e. strongly coupled data assimilation

Reanalysis:

- 96 members
- Daily data: Atmosphere, surface fluxes, surface ocean, OBGC
- Monthly data: subsurface ocean, sea ice, land

Forecasts:

- 10 members; 10 year leadtime; initialised every November 1960 present (wmo submission)
- currently extended to 96 members; 10 year leadtime; initialised every May and November 2003 present

Primary references:

- O'Kane et al (2021) CAFE60v1: A 60-year large ensemble climate reanalysis. Part I: System design, model configuration and data assimilation.
  J. Climate vol 34, 5153–5169, doi:10.1175/JCLI-D-20-0974.1

- O'Kane et al (2021) CAFE60v1: A 60-year large ensemble climate reanalysis. Part II: Evaluation
  J. Climate, vol 34, 5171–5194, doi:10.1175/JCLI-D-20-0518.1

Data published at

- Amazon Web Services (AWS): https://registry.opendata.aws/csiro-cafe60/

- CSIRO Data Portal: http://hdl.handle.net/102.100.100/389002?index=1

Background studies:

- T.J. O'Kane, P.A. Sandery, D.P. Monselesan, P. Sakov, M.A. Chamberlain, R.J. Matear, M.A. Collier, D.T. Squire and L. Stevens (2019) "Coupled data assimilation and ensemble initialization with application to multi-year ENSO prediction", J. Climate, 32, 997—1024

- T.J. O'Kane, P.A. Sandery, V. Kitsios, R.J. Matear, T. Moore, J.S. Risbey, I. Watterson (2020) Enhanced ENSO prediction via augmentation of multi-model ensembles with initial thermocline perturbations. (J. Climate, 33, pp2281–2293)

- P.A. Sandery, T.J. O'Kane, V. Kitsios and P. Sakov (2020) State estimation of the climate system with the EnKF using variants of coupled data assimilation (Mon. Wea. Rev.,148 (6), 2411-2431)

Model

- The atmospheric radiative forcing data used is based on CM2.1 CMIP5 historical forcings and was provided courtesy of GFDL
- This data was extended using RCP4.5 forcings for all the major radiative gases i.e. CO2, CH4, N2O etc, and aerosols
- The only fields that change at different dates are volcanic sulphate aerosols, stratospheric O3 and ocean CO2 used to estimate ocean carbon
- For O3 we used the spatially heterogeneous CMIP6 data which we tested this against the CMIP5 zonal mean O3 over various assimilation periods finding better results i.e. lower RMS error.
- Volcanic emissions post 2000 were based on a “neutral” year
- Ocean CO2 was based on data used in the ACCESS CMIP6

Observations

Table 1: Observation type and error estimates

Obs type	Dataset	spatial distribution	error estimate	R-Factor
Sea surface temperature SST	HadISST, OSISST, AVHRR, AMSR-E, AMSR-2, VIIRS, WindSat	point	0.5K, 0.5K, †, 0.5K, †, 0.25K, †	8
Sea level anomaly SLA	RADS	track	†	64
In situ ocean temperature TEM*	Argo, XBT, CTD, TAO, PIRATA	profiles	0.5K	8
In situ ocean salinity SAL*	Argo, CTD, TAO, PIRATA	profiles	0.075psu	8
Sea ice concentration SIC	HadISIC, OSISAF	gridded	0.1 [C], 0.1 [C]	8
Sea ice temperature SIT	HadISIT	gridded	0.1K	8
Zonal wind ARU	JRA55	gridded	$1ms^{-1}$	8
Meridional wind ARV	JRA55	gridded	$1ms^{-1}$	8
Air temperature ART	JRA55	gridded	1K	8
Specific humidity ARH	JRA55	gridded	0.05kg/kg	8

Table 2: *

* Low confidence CORA5.0 in situ data TEM2 & SAL2 have twice the error and four times the R-Factor to the high confidence data listed in the table.† error provided by vendor.

CORA5.0

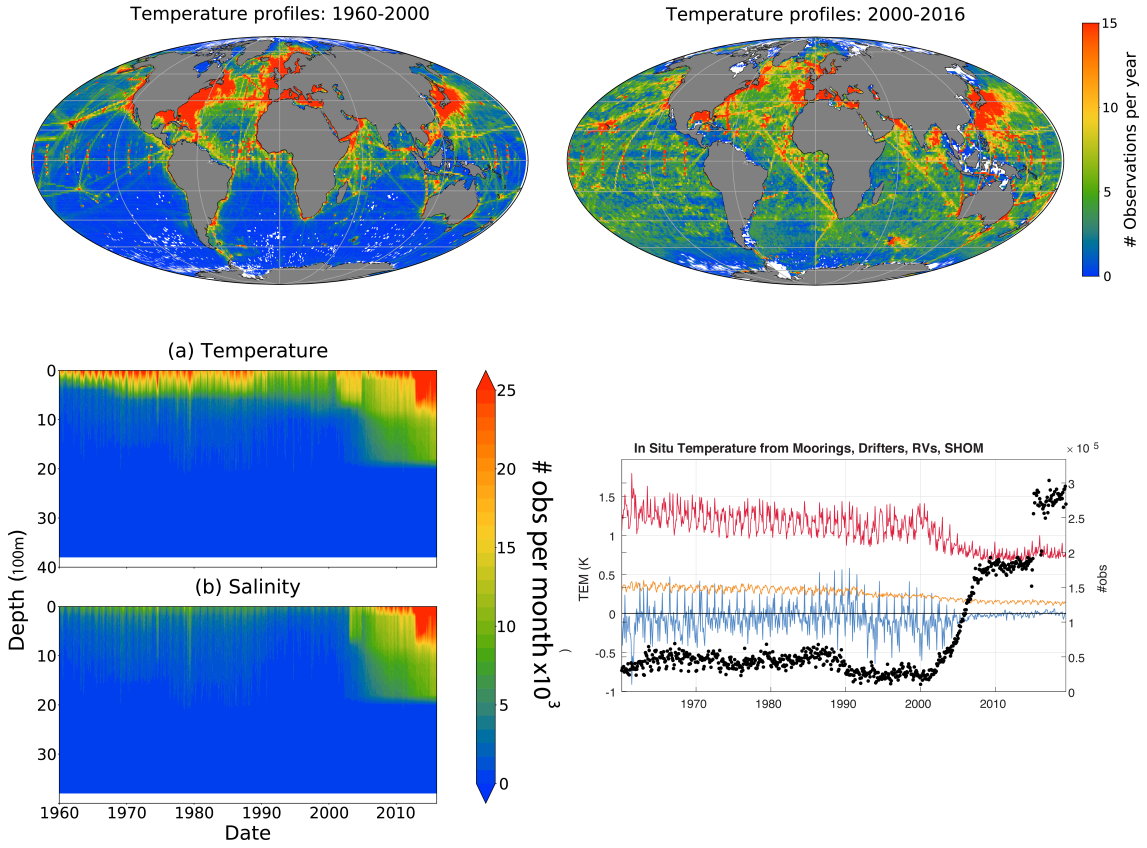

Figure 1:

EnKF scheme

The ETKF propagates first and second moments of $\mathbf{x}$ recursively and applies k-ensemble forecast and analysis anomalies $\mathbf{z}_i$ for $i = 1, 2, \ldots, k$ defined as

$$\mathbf{Z}^f = \frac{1}{\sqrt{k-1}}[\mathbf{z}_1^f, \mathbf{z}_2^f, \ldots, \mathbf{z}_k^f], \tag{1a}$$

$$\mathbf{Z}^a = \frac{1}{\sqrt{k-1}}[\mathbf{z}_1^a, \mathbf{z}_2^a, \ldots, \mathbf{z}_k^a] \tag{1b}$$

and where the state vectors are $\mathbf{z}_i^f = \mathbf{x}_i^f - \langle \mathbf{x}^f \rangle$ and $\mathbf{z}_i^a = \mathbf{x}_i^a - \langle \mathbf{x}^a \rangle$ which are n-dimensional in model space. The ETKF acts to choose appropriate initial forecast anomalies consistent with error covariance update equations within the vector subspace of ensemble anomalies formed as $\mathbf{P}^f = \mathbf{Z}^f \mathbf{Z}^{f^T}$ and $\mathbf{P}^a = \mathbf{Z}^a \mathbf{Z}^{a^T}$ and where the covariance update is given by

$$\mathbf{P}^a = (\mathbf{I} - \mathbf{K}\mathbf{H})\mathbf{P}^f, \tag{2a}$$

$$\mathbf{K} = \mathbf{P}^f \mathbf{H}^T (\mathbf{H}\mathbf{P}^f \mathbf{H}^T + \mathbf{D})^{-1} \tag{2b}$$

where $\mathbf{K}$ is the $n \times p$ Kalman gain, $\mathbf{P}$ is the positive definite state covariance error matrix, $\mathbf{I}$ is the indentity matrix, and $\mathbf{H}$ is the $p \times n$ linearised observational operator mapping forecast grid point values onto observational points.

ETKF cont...

The Kalman gain $\mathbf{K}$ acts on the innovation $\left[\mathbf{d}_i - \mathbf{H}\langle\mathbf{x}^f\rangle\right]$ and specifically i.e.,

$$\mathbf{x}^a = \mathbf{x}^f + \mathbf{K}\left[\mathbf{d} - \mathbf{H}\mathbf{x}^f\right] \tag{3}$$

$$\mathbf{Z}^a = \mathbf{Z}^f\mathbf{T} \tag{4}$$

where the transform matrix $\mathbf{T}$ is now defined in terms of the $k \times (k-1)$ matrix of non-zero eigenvalues such that

$$\mathbf{T} = \mathbf{C}(\mathbf{\Gamma} + \mathbf{I})^{1/2}\mathbf{C}^T \tag{5}$$

where the $\mathbf{\Gamma}$ (non-zero eigenvalues) is $(k-1) \times (k-1)$ and $\mathbf{C}$ is $k \times (k-1)$, corresponds to the transform matrix in spherical simplex form.

CAFE60 uses monthly mean observations and background (forecast) covariances to update the state estimates. For the atmosphere we seek to constrain only the large scale structures i.e.jet, Hadley and Ferrel cells etc.

- We also employ SST bias correction (AR1 function), covariance localization, etc..

- EnKF-C, adaptively moderates the impact of observations of various types using two parameters, the so-called R- and K-factors (Sakov and Sandery 2017).

- The K-factor, limits the impact of individual observations i.e, those with large innovations likely to be inconsistent with the state of the DA system, by smoothly increasing observation error variance depending on the projected increment such that the resulting increment does not exceed the estimated state error times K.

- A further benefit of the method is that it minimizes the innovations by modifying the distribution of observation error to better match the distribution of model error, thereby increasing the gain and the observation impact.

- R-factors are defined for each observation type and represent scaling coefficients for the corresponding observation error variances (Sandery et al. 2020).

Table 3: P.A. Sandery, T.J. O'Kane, V. Kitsios and P. Sakov (2020) State estimation of the climate system with the EnKF using variants of coupled data assimilation (EOR Mon. Wea. Rev.)

case	A-A	A-O	O-O	O-A	Atmospheric Increment	Ocean Increment	Type
1	1	1	1	1	atmospheric and ocean observations	atmospheric and ocean observations	strong
2	0	0	1	1		atmospheric and ocean observations	strong
3	1	1	0	0	atmospheric and ocean observations		strong
4	1	0	1	0	atmospheric observations	ocean observations	weak
5	0	0	1	0		ocean observations	weak
6	1	0	0	0	atmospheric observations		weak
7	0	1	0	1	ocean observations	atmospheric observations	strong
8	0	1	1	0	ocean observations	ocean observations	strong
9	1	0	0	1	atmospheric observations	atmospheric observations	strong
10	0	0	0	1		atmospheric observations	strong
11	1	1	1	0	atmospheric and ocean observations	ocean observations	strong
12	0	1	1	1	ocean observations	atmospheric and ocean observations	strong
13	0	1	0	0	ocean observations		strong
14	1	1	0	1	atmospheric and ocean observations	atmospheric observations	strong
15	1	0	1	1	atmospheric observations	atmospheric and ocean observations	strong
16	0	0	0	0			control

- A-A atmospheric covariances
- O-O ocean covariances
- A-O atmosphere-ocean cross-covariance: atmospheric increment due to ocean observations
- O-A ocean-atmosphere cross-covariance: ocean increment due to atmospheric observations

Ocean error growth: 7 day cycle

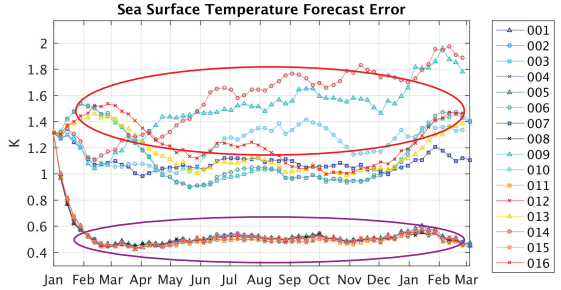

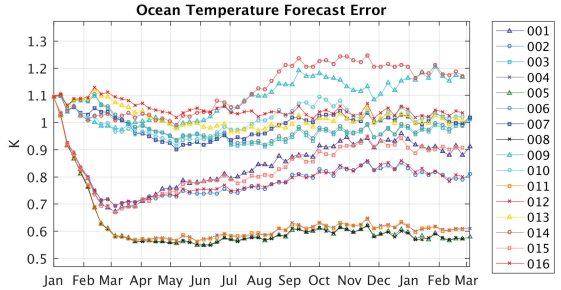

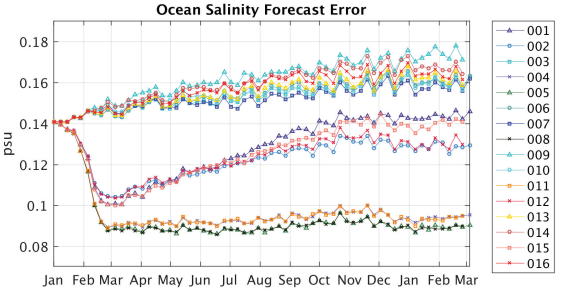

Global forecast innovation errors..

$$\sigma_G(T) = \frac{1}{T}\ln\left(\frac{\sigma_F(T)}{\sigma_A}\right)$$

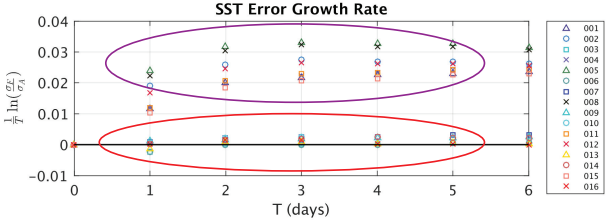

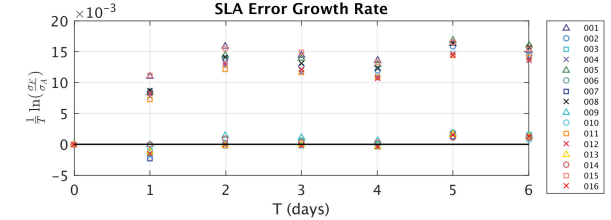

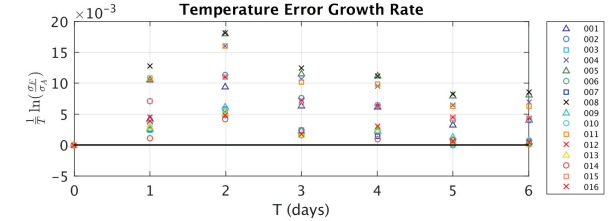

Error growth rates for (a) sea surface temperature, (b) sea-level anomaly and (c) in-situ temperature.

Small innovation - error growth as skill decreases w.r.t. time

Large innovation - saturated errors

Table 4: Ocean domain

1st class	2nd class	3rd class	4th class
008: A-O, O-O	002: O-A, O-O	001: A-A, A-O, O-O, O-A	remaining variants saturated
005: O-O	012: A-O, O-O, O-A	011: A-A, A-O, O-O	
		015: A-A, O-O, O-A	

Table 5: Atmosphere domain

1st class	2nd class
001: A-A, A-O, O-O, O-A	remaining variants saturated
008: A-O, O-O	
011: A-A, A-O, O-O	
003: A-A, A-O	
009: A-A, O-A	

In the atmosphere domain and for a 7-day or longer cycle, an atmospheric increment based on ocean observations performs almost as well as directly assimilating atmospheric observations.

- A-A atmospheric covariances
- O-O ocean covariances
- A-O atmosphere-ocean cross-covariance: atmospheric increment due to ocean observations
- O-A ocean-atmosphere cross-covariance: ocean increment due to atmospheric observations

In addition CAFE60 has sea ice DA strongly coupled to the ocean. OBGC is weakly coupled to the ocean via the cross domain covariance dependent on ocean observations. No assimilation of land based observations. Current system now assimilates GRACE soil moisture data.

Atmosphere

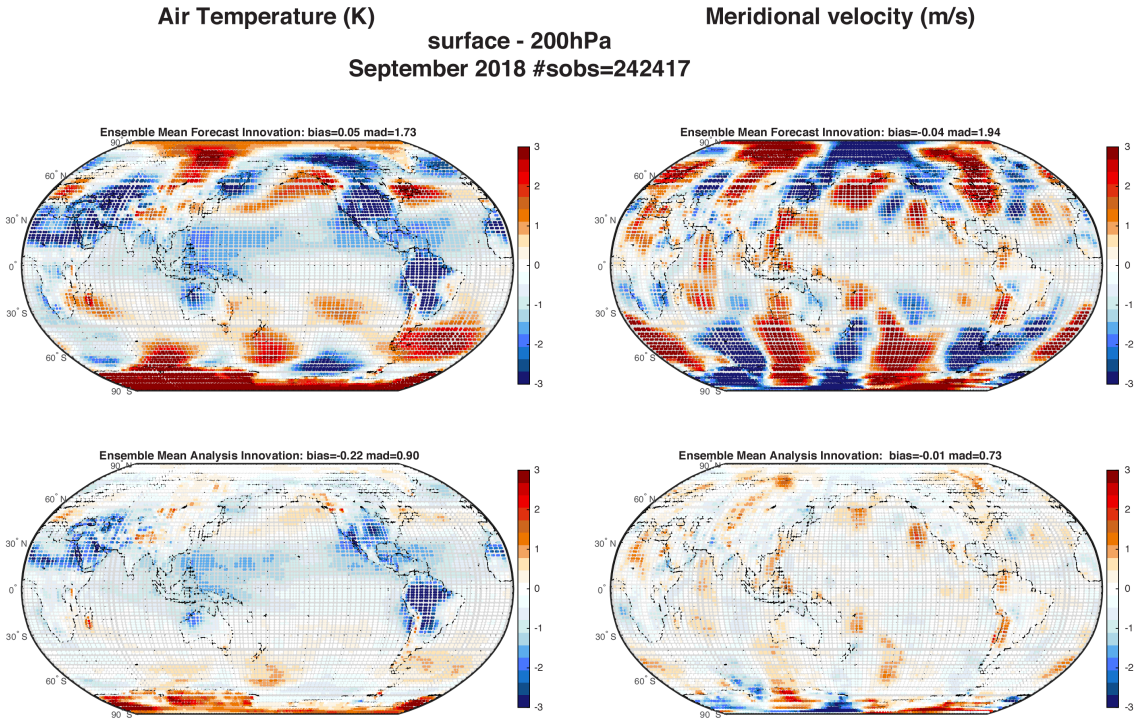

Figure 2:

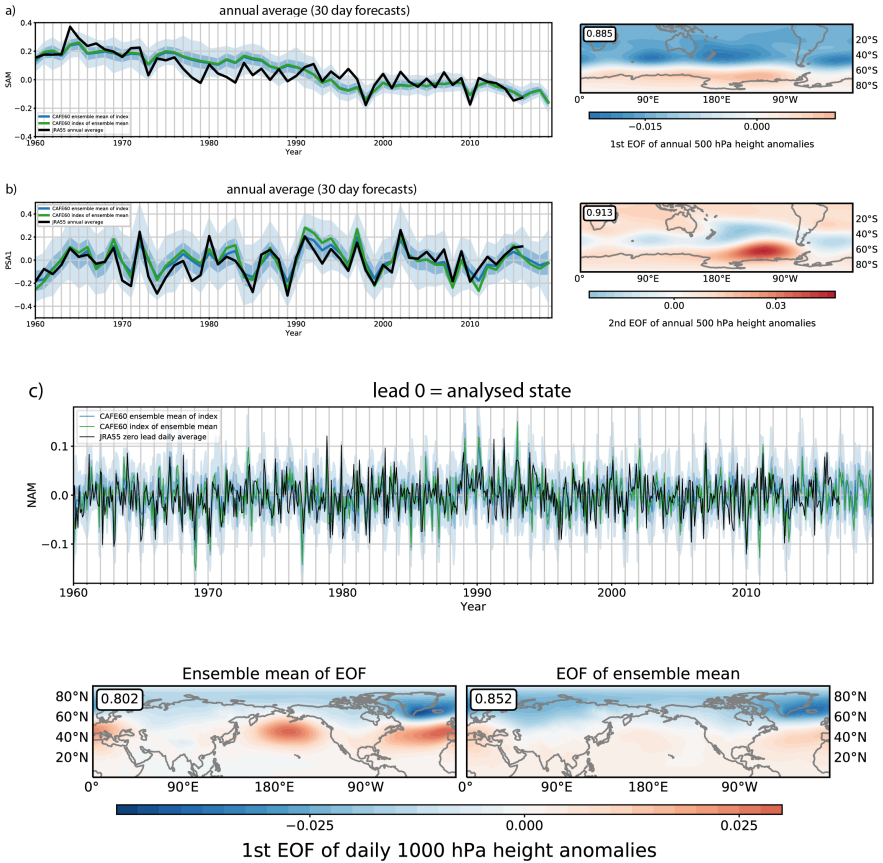

Figure 3: (a) Annual means of the CAFE60 SAM index calculated as the leading PC of daily 500hPa geopotential height data and the corresponding EOF1 spatial pattern and its correlation with JRA55. (b) Similar calculations for the annual mean PSA1 mode and (c) the Northern Annular mode / Arctic Oscillation EOF-based index for lead-zero daily PCs and corresponding EOF patterns. Here, both the ensemble mean of the EOF patterns and the EOF pattern of the ensemble mean are shown to illustrate model bias in the Pacific Ocean evident in the ensemble mean of member EOFs which are not evident whenconsidering the EOF of the ensemble mean.

IPO-TPI

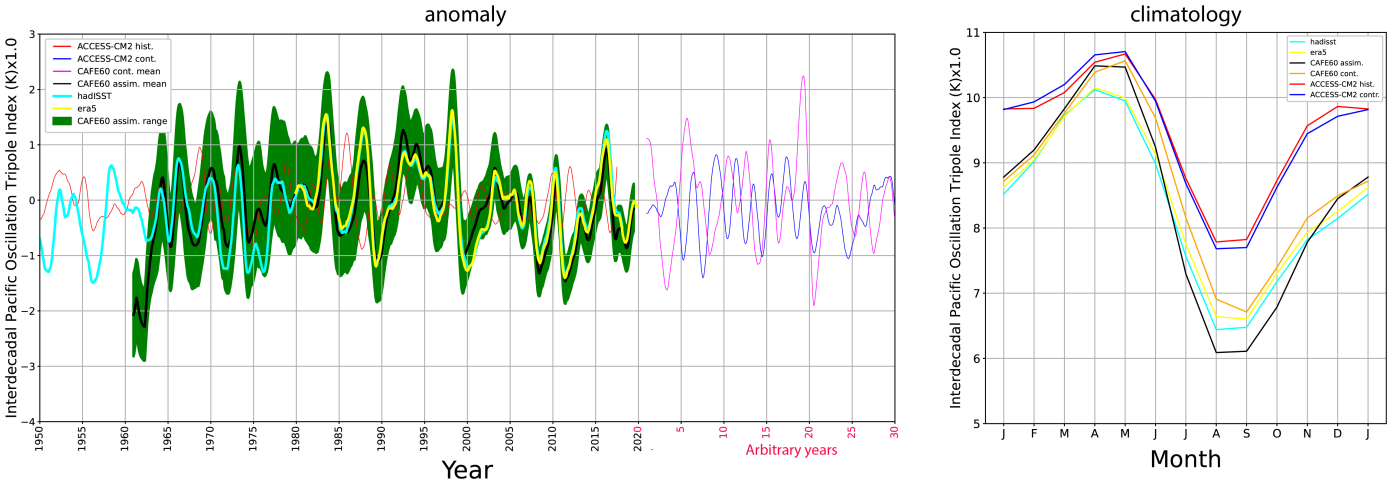

Figure 4: Interdecadal Pacific Oscillation tripole index.

MJO

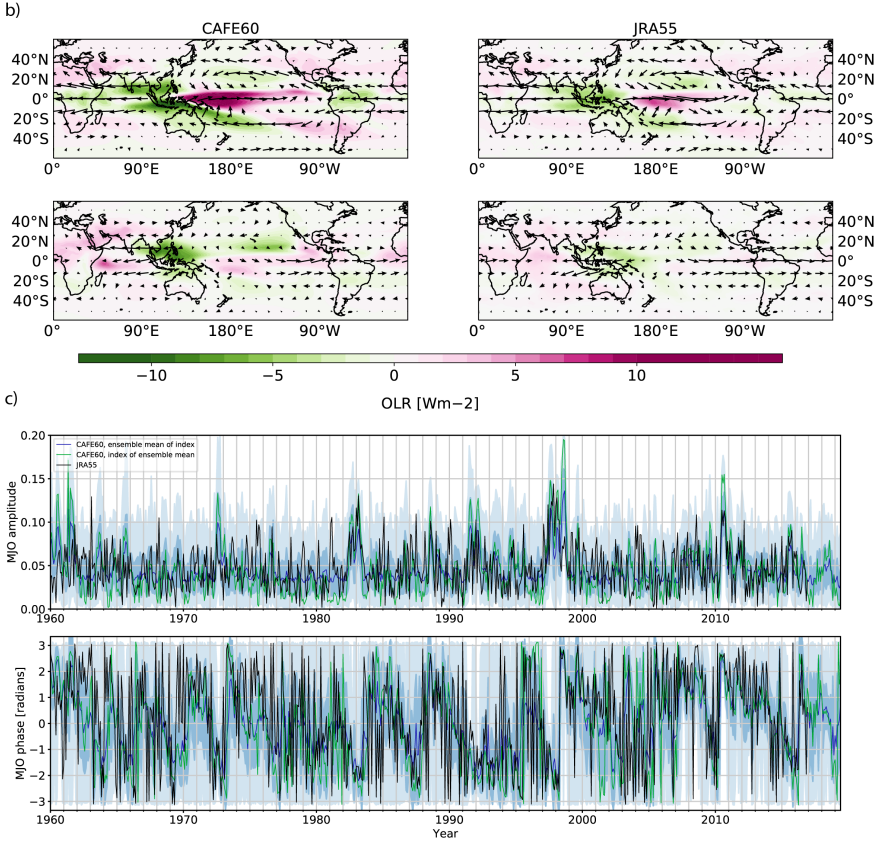

Figure 5: (b) The two leading principal components (PCs) of the daily 850 minus 150-hPa global velocity potential and their regression onto OLR and the ensemble mean wind direction pattern resulting from the regression of PCs onto u and v wind anomalies at 150 hPa. (c) Time series of amplitude and phase of the MJO in terms of daily 850 minus 150-hPa global velocity potential. Light blue shading indicates the CAFE60 ensemble spread, the darker blue shading indicates one standard deviation from the mean.

SAT and Precipitation

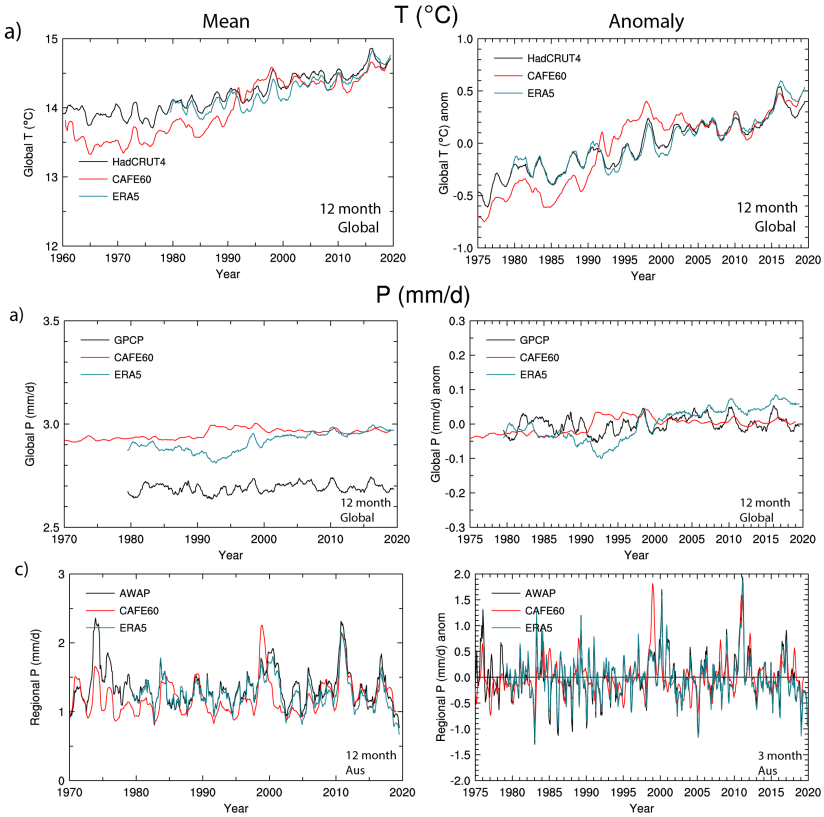

Figure 6: Comparison of CAFE60 ensemble mean precipitation and surface air temperature to HadCRUT4, ERA5, GPCP and AWAP.

Ertel PV

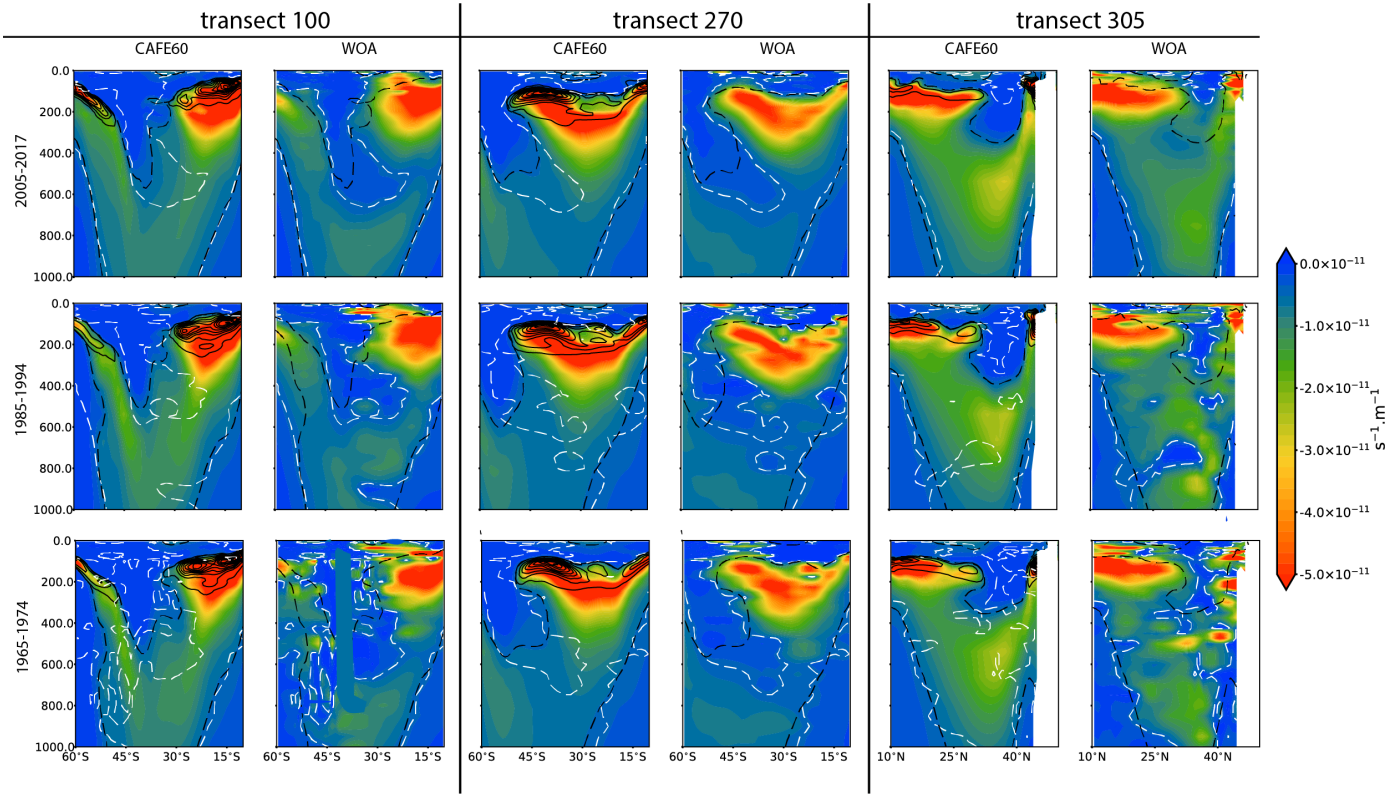

Figure 7:

Global MOC

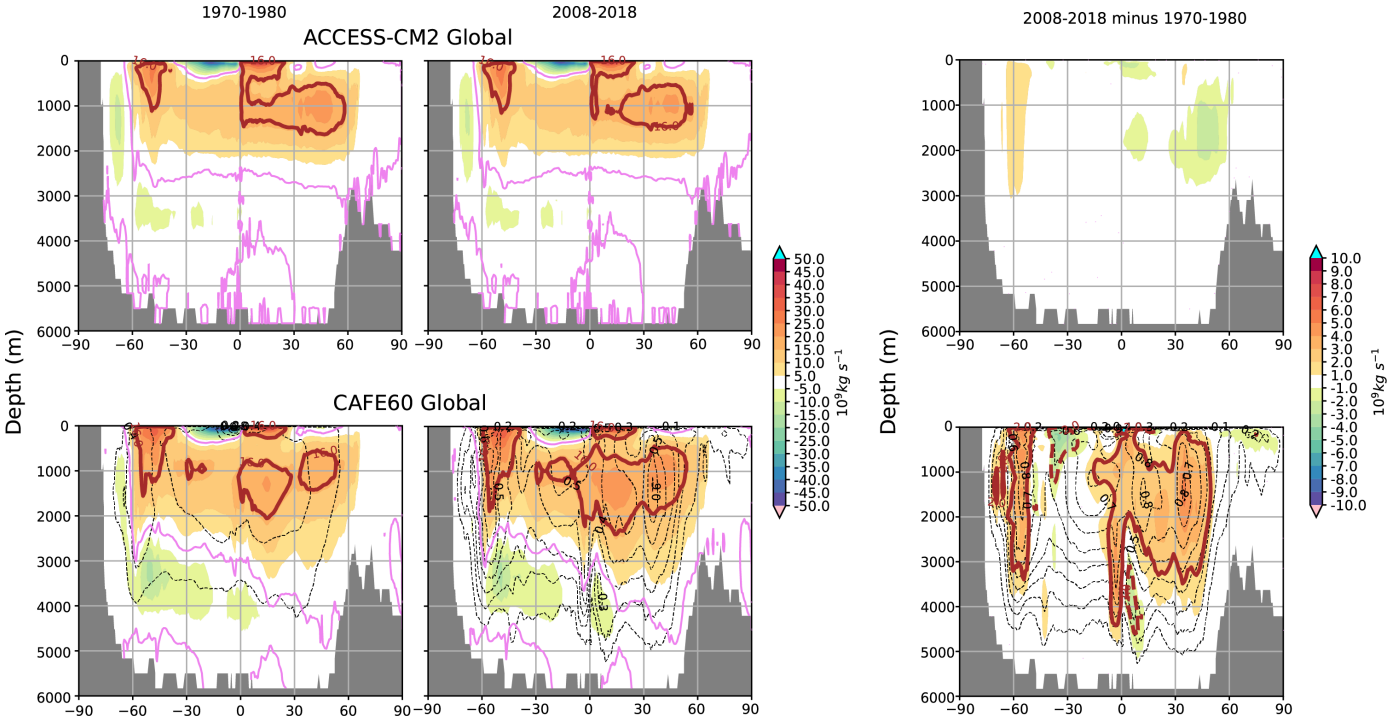

Figure 8: ACCESS-CM2 and CAFE60 meridional volume transport in depth coordinates defined in terms of the mass transport (kgs^{-1}) as a function of horizontal location and depth. Here the MOC are defined globally. Red contours indicate 16Sv and 2 Sv respectively. Black contours indicate stddvn.

Transports

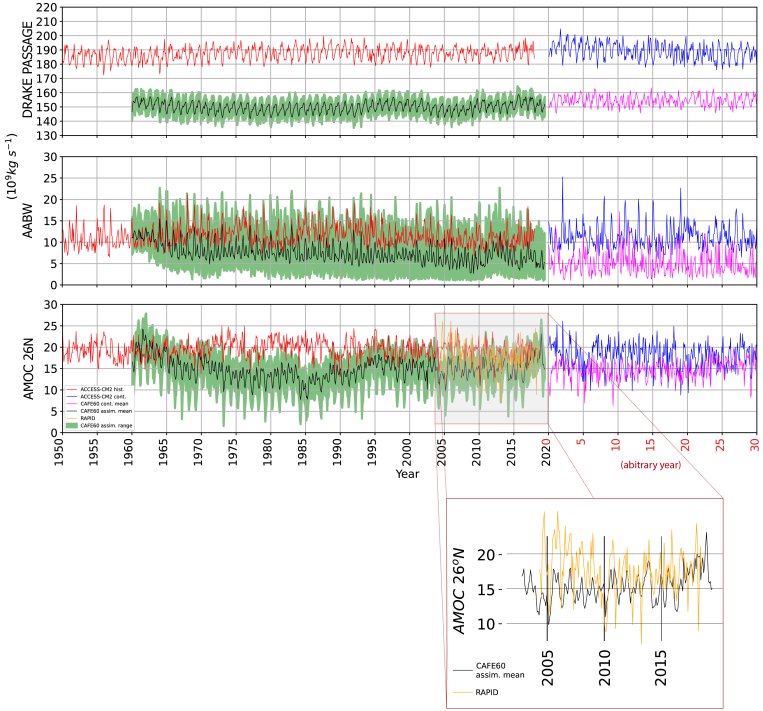

Figure 9: To obtain strength of overturning for a particular common index to compare to generally very limited observations, we simply identify the maximum value within a particular depth and latitude box, the range of these boxes are: $AMOC26^\circ N - 25.5^\circ - 26.5^\circ, 0 - 6000m$ $AABW90^\circ S - 60^\circ S, 0 - 3000m$ Note that $AMOC26N$ is identified at the two longitudes 25.5 and 26.5 that span the reqired $26^\circ N$.

Sea Ice Extent

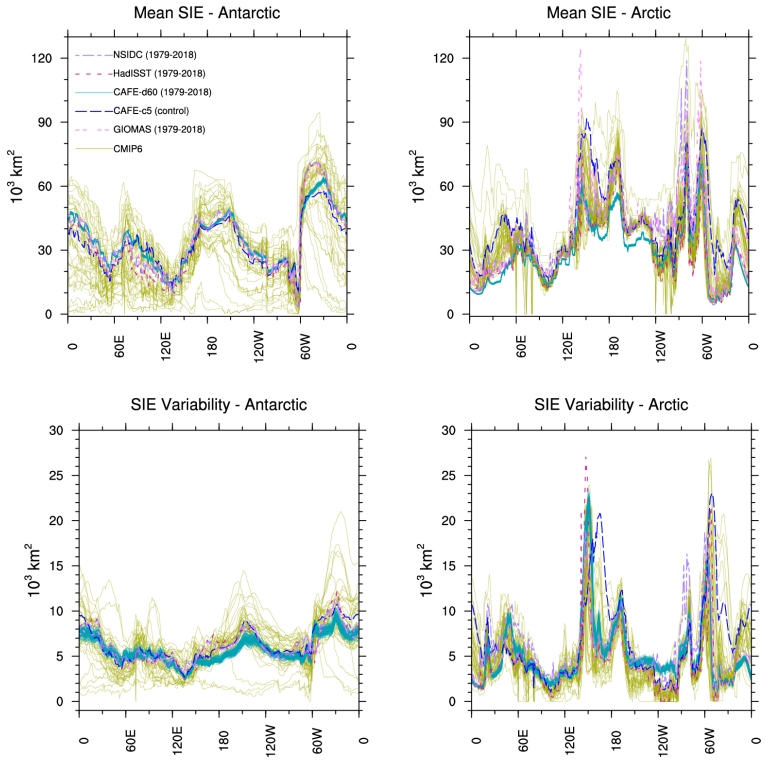

Figure 10: Arctic sea ice in JUL-SEP unrealistically low. Variability is good but trends are poor. Sea Ice is a huge challenge for long cycle length!

Soil moisture DA

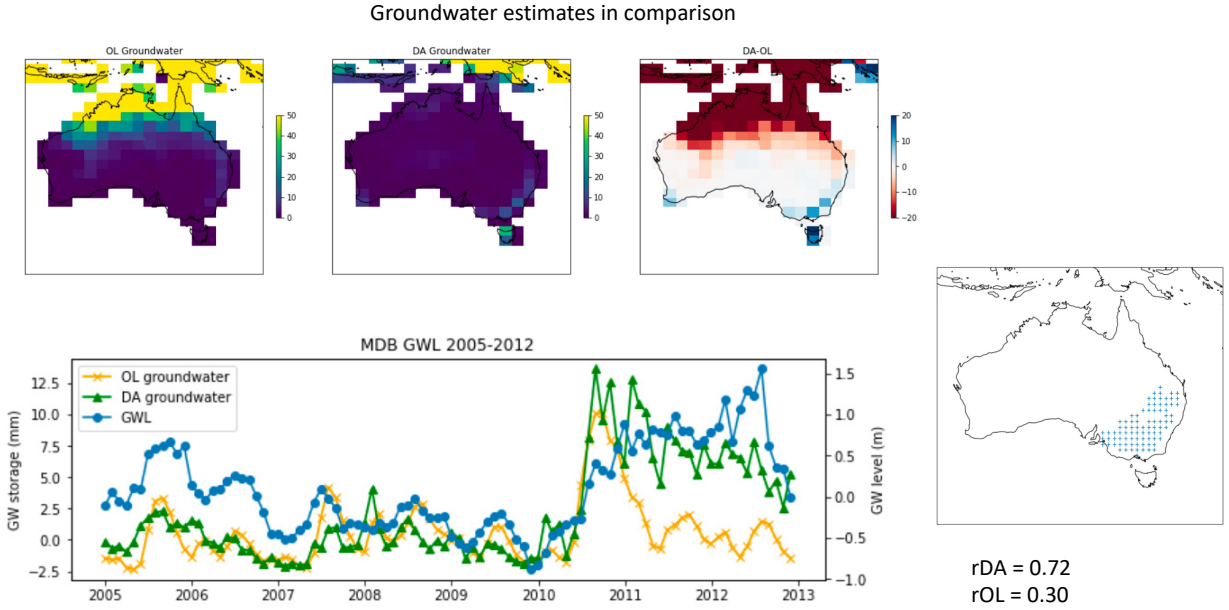

Figure 11: Impact of soil moisture DA on groundwater estimation.

Summary

Challenges:

- Sea Ice
- blocking over Euro-Atlantic sector
- pre-Argo ocean

Recent advances:

- Improved Arctic sea ice - model parameterizations, ice thickness assimilation
- Assimilation of soil moisture content from GRACE

CAFE60 offers a novel way to understand climate variability and predictability over the last 6 decades.

Thank You

CSIRO Oceans & Atmosphere

Terence O'Kane

t +61 3 6232 5066

e terence.okane@csiro.au

w http://people.csiro.au/O/T/Terence-OKane